*Journal of GeoEngineering, Vol. 17, No. 1, pp. 023-032, March 2022*
*http://dx.doi.org/10.6310/jog.202203_17(1).3*



# A COMPARATIVE REVIEW ON LIQUEFACTION POTENTIAL OF KATHMANDU LACUSTRINE DEPOSITS BASED ON THE PREDICTED LIQUEFACTION SITES AND LOCATIONS OBSERVED DURING THE 2015 GORKHA EARTHQUAKE

Mandip Subedi [1*] and Indra Prasad Acharya [2]

## ABSTRACT

In Nepal, historic earthquakes have shown extensive liquefaction in different areas of the country, including its capital, Kathmandu Valley. The 1833 and 1934 earthquakes caused significant harm due to liquefaction. An earthquake of moment $M_w$7.8 struck on 25 April, 2015, keeping the epicentre at the central part of Nepal. Although damages due to liquefaction were limited, several surface manifestations were observed at various places in the valley. This paper summarises the field reconnaissance concerning the liquefaction cases in Kathmandu after the mainshock. The field observations, alongside results from liquefaction evaluation, contrasts with the previous liquefaction studies conducted before the 2015 Earthquake for the valley. To evaluate the irregularity of existing maps with the ground manifestations caused by the 2015 Gorkha earthquake, we utilised the geotechnical database gathered from 400 locations before the quake and 10 boreholes drilled before the 2015 Gorkha earthquake to conduct quantitative analyses and modelling using simplified procedure by Idriss and Boulanger (2008). Likewise, the susceptibility of affected zones to liquefaction during the 2015 Gorkha earthquake is depicted, and utilized standard technique is validated to estimate liquefaction hazard in Kathmandu Valley.

*Key words:* 2015 Gorkha earthquake, predicted liquefaction, observed liquefaction, Kathmandu Valley.

## 1. INTRODUCTION

Recent global earthquakes have demonstrated the significant damage caused by liquefaction (Koseki *et al.* 2015). In Nepal, recorded earthquakes of 1408, 1833 ($M_L$7.7), 1934 ($M_w$8.1), and 1988 ($M_w$6.8) triggered liquefaction events in various locations of the country, including its capital, Kathmandu Valley. On 25 April 2015, earthquake of magnitude $M_w$7.8 hit the eastern edge of 800 km wide seismic gap, triggering ground failures in the valley (Sharma *et al.* 2016, 2018a, and 2018b). Although damages due to liquefaction were limited, several surface manifestations like ground fissures, sand boils were seen at various places in the valley (Subedi *et al.* 2018; Gautam *et al.* 2017; Sharma *et al.* 2019; KC *et al.* 2019; Jha *et al.* 2020; Subedi *et al.* 2021).

Ample amount of studies are carried out on the topic of liquefaction hazard in Kathmandu Valley recently, however the studies conducted by UNDP (1994), JICA (2002), and Piya (2004) are notable ones. JICA conducted a study of liquefaction in 2002 and found that most of the area in Kathmandu was least susceptible to liquefaction. Similarly, UNDP (1994) and Piya (2004) both followed similar analysis techniques. The former followed the qualitative analysis technique for determining the liquefaction score, while the latter used boreholes data to verify qualitative analysis results quantitatively. However, UNDP (1994) and Piya (2004) reported that most of the areas in Kathmandu Valley are vulnerable to liquefaction; unlike, the JICA (2002) map's indication that the majority of the valley is not susceptible to liquefaction. The liquefaction maps are contrasting with each other and more importantly, all these studies are based on very primitive techniques, which have also been revised with time. Thus, it is imperative to reassess the existing liquefaction hazard maps with the help of field observations of liquefaction during the 2015 Gorkha earthquake using recent liquefaction assessment technique.

This paper summarizes the field reconnaissance concerning the Kathmandu Valley liquefaction cases after the mainshock of the 2015 Gorkha earthquake. The field observations, alongside results from liquefaction evaluation using simplified method given by Idriss and Boulanger (2008), are contrasted to the widely used liquefaction hazard maps made by UNDP (1994), JICA (2002), and Piya (2004). To assess the irregularity of existing maps with the ground manifestations caused by the 2015 Gorkha earthquake, we used 1510 boreholes data (Fig. 1(a)) along with numerical analyses, field examinations, and laboratory investigations. The geotechnical characterization of the valley and a portrayal of the liquefaction susceptibility of affected zones during the Gorkha earthquake are performed. In addition, this study assessed the applicability of broadly utilized standard technique to estimate liquefaction hazard in Kathmandu Valley. From observations and liquefaction assessment results, the existing hazard maps found unrepresentative and underestimated the susceptibility of liquefaction in Kathmandu Valley.

Manuscript received July 23, 2021; revised September 30, 2021; accepted November 7, 2021.

[1*] Ph.D. (corresponding author), Department of Civil Engineering, Pulchowk Campus, Institute of Engineering, Tribhuvan University, Nepal (e-mail: mandip.072phce104@ioe.edu.np).
[2] Associate Professor, Department of Civil Engineering, Pulchowk Campus, Institute of Engineering, Tribhuvan University, Nepal.

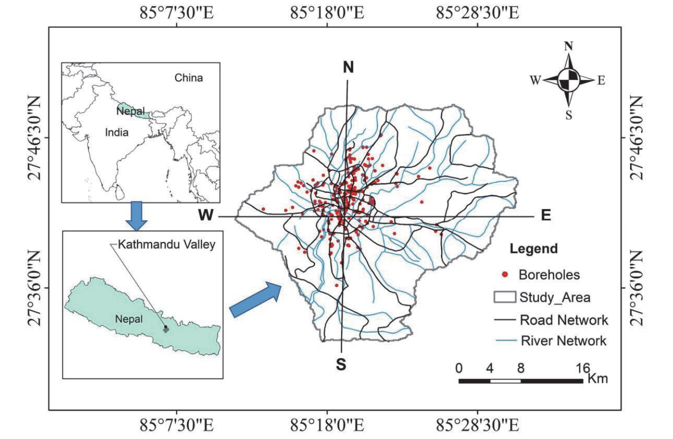


(a) Map showing location of the study area with all borehole locations

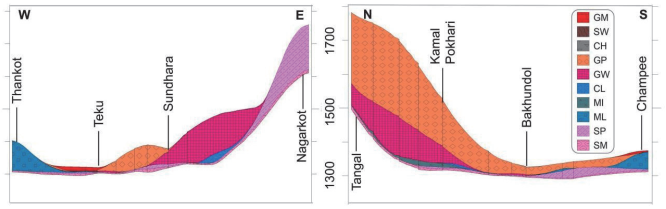


(b) Schematic east-west and north-south stratigraphic cross-sections of the valley

**Fig. 1 Location map of the study area with cross-sectional profiles**

## 2. STUDY AREA

### 2.1 Geological Aspects

The bowl-shaped Kathmandu Valley is mostly flat on its terrain except for some gorges created by river networks within the valley. It consists of lacustrine deposits surrounded by high hills underlain by basement rocks varying in depth. The schematic stratigraphic cross-sections of the valley prepared using the borehole logs are shown in Fig. 1(b). Moribayashi and Maruo (1980) calculated the maximum depth of the Kathmandu basin-fill sediments to be around 650 m based on gravity measurements. Quaternary sediments of the valley can be divided into Southern Group, Northern group, and Central. The southern group consists of a hilly terrace formed during the Pliocene to mid-Pleistocene. In comparison, the middle part consists of predominantly dark grey diatomaceous and carbonaceous beds of the lacustrine basin (Sakai 2001). Whereas, the top section is composed of fine to medium sand silt that is occasionally interspersed with fine gravels and clays. The northern part consists sand terrace from fluvial-lacustrine or fluvial deltaic origins (Sakai 2001).

### 2.2 Seismotectonic Setting

The Indian plate converges with the Eurasian plate at a rate of roughly 45 mm per year in a north-northeast direction, forming the Himalayas and Tibetan Plateau (Copeland 1997). Nepal lies within the collision zone of Indian and Eurasian Plates. Between these plates, the Himalayan arc serves as an active barrier, causing earthquakes in the regions with their periodic movements. The collision of the Indian and Eurasian plates results in the formation of active faults along key tectonic borders. The 2015 Gorkha earthquake and its subsequent aftershocks were also the consequence of thrust faulting between the subducting Indian plate and the northern Eurasian plate.

Nepal is located in one of the world's most seismically active areas, with a long history of earthquakes. It has felt the wrath of mega earthquakes around 11 times with an intensity of over $M_w$7.0 throughout history (Thapa *et al.* 2017). The most significant ones are the Nepal-Bihar Earthquake (1934, $M_w$8.1) and the Gorkha earthquake (2015, $M_w$7.8). The spatial distribution of earthquakes in Nepal during 1255-2015 AD is presented in Fig. 2.

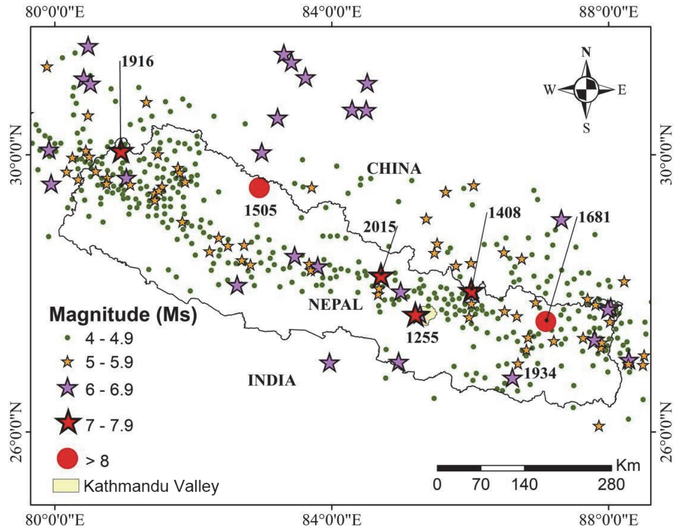


**Fig. 2 Spatial distribution of earthquakes with magnitude Ms ≥ 4.0 during 1255-2015 AD in Nepal (redrawn after Thapa *et al.* 2017)**

## 3. MATERIAL AND METHODS

### 3.1 Borehole Data

For this study, we drilled 5 boreholes at 2015 Gorkha earthquake liquefied sites, 2 boreholes at 1934 Bihar-Nepal Earthquake liquefied sites and 3 boreholes at central valley. Moreover, 1500 boreholes from 400 various locations as secondary data were collected, analysed, and modelled for geotechnical characterization of the valley. Likewise, numerical analysis, field examinations, and laboratory investigations were performed to portray the liquefaction vulnerability of affected zones in the Gorkha earthquake. Particle size distribution and plasticity chart are made to check the basic scenario of liquefaction in the valley. The variation of groundwater table of the study area analyzed from four sources, *i.e.,* borehole data, measurement of groundwater table of prevailing tube well and dug wells by Pathak *et al.* (2009), and groundwater monitoring wells in Kathmandu groundwater basin by Nepal Water Supply Corporation (NWSC).

### 3.2 Factor of Safety (FS) against Liquefaction

The factor of safety (FS) against liquefaction based on Idriss and Boulanger (2008) was determined using Eq. (1):

$$FS = \frac{CRR}{CSR} = \frac{CRR_{7.5} \times MSF \times K_\sigma}{CSR} \tag{1}$$

where $CRR_{7.5}$ is the calculated CRR for the earthquake of $M_w7.5$; MSF is a magnitude scaling factor that takes the impacts of shaking time into consideration, and $K_\sigma$ is a component that contributes to the occurrence of prolonged static shear stresses, such as those found beneath foundations or on slopes.

MSF and $K_\sigma$ were evaluated as follows (Eqs. (2) and (3)):

$$\text{MSF} = 6.9\, e^{-\frac{\text{Mw}}{4}} - 0.058 \quad (\leq 1.8) \tag{2}$$

$$K_\sigma = 1 - C_\sigma \ln\left(\frac{\sigma'_v}{P_a}\right) \leq 1.1 \tag{3}$$

$$C_\sigma = \frac{1}{18.9 - 2.55\sqrt{(N_1)_{60cs}}} \leq 0.3 \tag{4}$$

The SPT-N derived from the field investigation was deployed to calculate CRR. Equation (5) shows the correction process:

$$(N_1)_{60} = NC_N\, C_S\, C_B\, C_E\, C_R \tag{5}$$

where

$(N_1)_{60}$ is the SPT blow count normalized to an overburden pressure of 100 kPa (*i.e.,* atmospheric pressure) with a hammer efficiency of 60%.
$N$ is the measured SPT.
$C_N$ is the correction factor for overburden stress.
$C_S$ is the correction factor for samplers with and without liners.
$C_B$ is the correction factor for borehole diameter.
$C_E$ is the correction factor for the hammer energy ratio.
$C_R$ is the correction factor for rod length.

The $CRR_{7.5}$ is calculated using Eq. (6).

$$\text{CRR}_{7.5} = \exp\left(\left(\frac{(N_1)_{60cs}}{14.1}\right) + \left(\frac{(N_2)_{60cs}}{126}\right)^2 - \left(\frac{(N_3)_{60cs}}{23.6}\right)^3 + \left(\frac{(N_4)_{60cs}}{25.4}\right)^4 - 2.8\right) \tag{6}$$

where $(N_1)_{60cs}$ is an equivalent clean-sand SPT blow count. Equations (7) and (8) are used to calculate $(N_1)_{60cs}$:

$$(N_1)_{60cs} = (N_1)_{60} + \Delta\,(N_1)_{60} \tag{7}$$

$$\Delta\,(N_1)_{60} = \exp\left(16.3 + \frac{9.7}{\text{FC}+0.01} - \left(\frac{15.7}{\text{FC}+0.01}\right)^2\right) \tag{8}$$

where FC is the fines content in the soils obtained from sieve analysis of the borehole or split-spoon samples.

The CSR is evaluated as follows using Eq. (9):

$$\text{CSR} = 0.65\frac{\tau_{\max}}{\sigma'_{vc}} = 0.65\frac{\sigma_{vc}}{\sigma'_{vc}}\frac{a_{\max}}{\text{g}}r_d \tag{9}$$

where g is the acceleration due to gravity, $a_{\max}$ is the peak ground acceleration at the ground, $\sigma_{vc}$ and $\sigma'_{vc}$ are the total and effective overburden stress, respectively, and finally, $r_d$ is the stress reduction factor as calculated in Eq. (10):

$$r_d = \exp\left[-1.012 - 1.126\sin\left(\frac{z}{11.73} + 5.133\right) + M_W\left(0.106 + 0.118\sin\left(\frac{z}{11.28} + 5.142\right)\right)\right] \tag{10}$$

where $z$ is the depth of soil layer in meters.

### 3.3 Liquefaction potential index (LPI)

Liquefaction potential index (LPI) introduced by Iwasaki *et al.* (1982) is often used to quantify the severity of liquefaction at any location. It considers the effect of the liquefiable soil layer's width, depth, and FS, assuming that the severity of liquefaction is proportional to the thickness of the liquefied layer, its proximity to the ground surface, and the extent to which the FS is less than 1. The LPI is estimated by using Eq. (11) for the top 20 meters or less soil profile (Iwasaki *et al.* 1982).

$$\text{LPI} = \int_0^z F(z)\, W(z)\, dz \tag{11}$$

where $z$ = depth of layer; $F(z)$ = function of FS against liquefaction defined as,

$$F(z) = 1 \quad \text{for FS} \leq 1 \tag{12}$$

$$F(z) = 0 \quad \text{for FS} > 1 \tag{13}$$

$W(z)$ is a depth-weighting factor defined as

$$W(z) = 10 - 0.5z \tag{14}$$

## 4. RESULT

### 4.1 Geotechnical Analysis

The site assessment revealed that the majority of the soils in the Kathmandu Valley are clayey silt and silty sand. Analysing SPT data 1510 boreholes, the SPT values of soil layers lying in the central part were much lesser than the outer. About 85% of the borehole test data found to have SPT-N less than 20, and more than 50% have SPT less than 10 in shallow depth in the valley's core area. The average SPT-N of Kathmandu soil at depths 1.5m, 3m, 6m, 9m, and 15m found to be 12, 15, 18, 20, and 23, respectively. More than 40% of the borehole locations have liquid limit (LL) less or equals 35%. This whole scenario strongly indicates the high susceptibility of liquefaction in the Kathmandu Valley, especially in its central region. Figure 3 shows grain size distribution and plasticity chart (Fig. 3) for soil in Kathmandu Valley. Particle size distribution for soil finer than 75 µ is not available as hydrometer analysis to determine the particle size distribution of fine-grained soils (passing through 75 µ sieve) is rarely used in Nepal. Figure 3 reveals that soil samples contain significant portion of sand and silt. It supports the fact that Kathmandu Valley was once a lake and had a lacustrine and fluvial origin. Additionally, two distinct sets of particle size distribution curves illustrating distribution ranges for the potentially

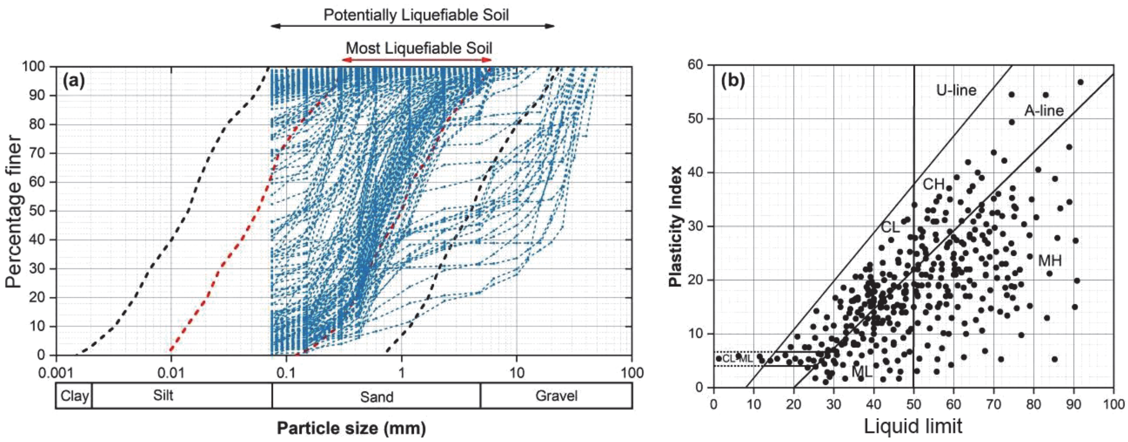


**Fig. 3 (a) The particle size distribution of Kathmandu soil with a range of potentially liquefiable and most liquefiable soils as suggested by Tsuchida and Hayashi (1972) and (b) plotting fine-grained soils in the plasticity chart given by Casagrande (1947)**

liquefiable and most liquefiable soils given by Tsuchida and Hayashi (1972) are also plotted (Fig. 3(a)). It shows that particle size distribution of the valley is higher inside the potentially liquefiable soil boundary and highest inside the edge of most liquefiable soil which clearly suggests that soil in Kathmandu has deposits that are very susceptible to liquefaction.

Moreover, the plasticity index is found in the range of 1.73 ~ 34, with most soils having 10 ~ 20 plasticity values as shown in Casagrande chart (Casagrande 1947) for all cohesive soils taken for this study (Fig. 3(b)). It reveals that the majority of fine-grained soils include silt with moderate to high swelling properties, which is essential for liquefaction evaluation since silts with low plasticity are often more sensitive to seismic motion (Bray and Sancio 2006). In addition, the number of data versus range of geotechnical properties values are shown in Fig. 4.

Studying water table became essential because it is a significant component in the occurrence of liquefaction in dynamic motion. The groundwater table (GWT) study was conducted using data from two sources, *i.e.,* borehole log information and groundwater table map prepared by Shrestha *et al.* (2016). About eighty percent of the total rainfall in Kathmandu Valley occurs during the monsoon (June to September) season. Several studies reported significant increment of ground water table in rainy season. The groundwater table is usually shallow in the valley during the rainy season, ranging from 0.5 and 5 meters below ground level (Fig. 5). The GWT in the dry season from January to May does not change significantly. Coincidently, the time of site investigations and earthquake event were in the dry season, and therefore the effect of GWT variation on the liquefaction assessment is supposed to be insignificant.

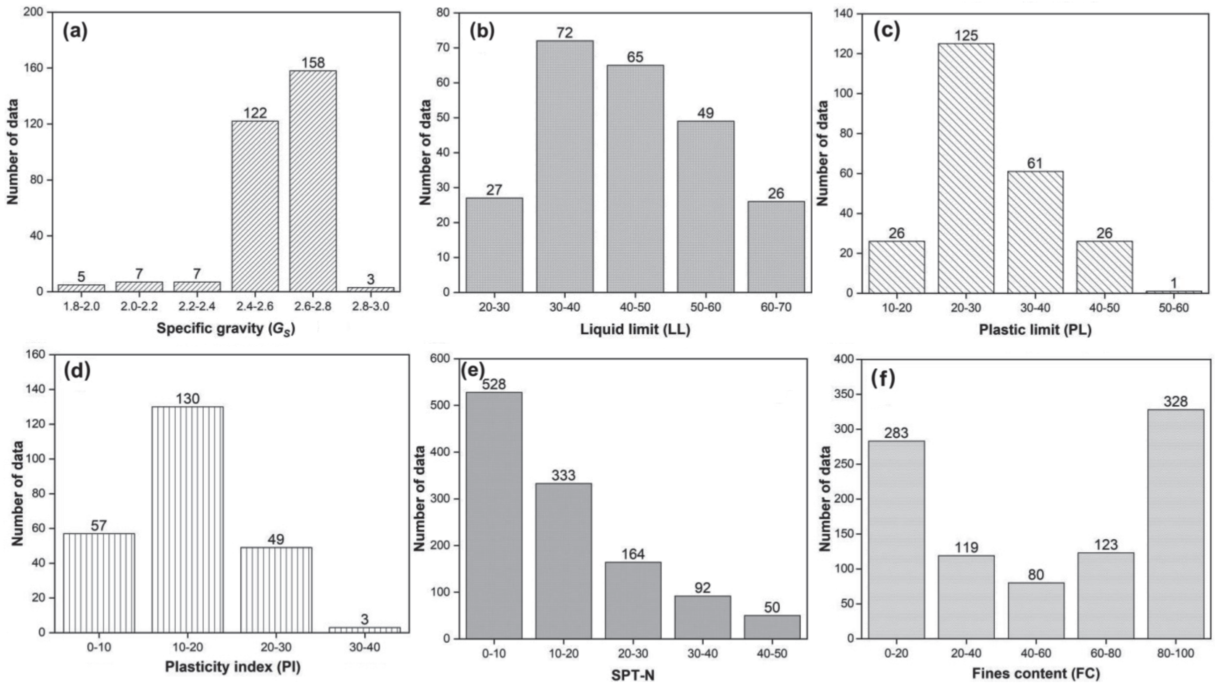


**Fig. 4 Geotechnical properties of the soil in the Kathmandu Valley: (a) specific gravity; (b) liquid limit; (c) plastic limit; (d) plasticity index; (d) SPT-N value; and (e) fines content (FC)**

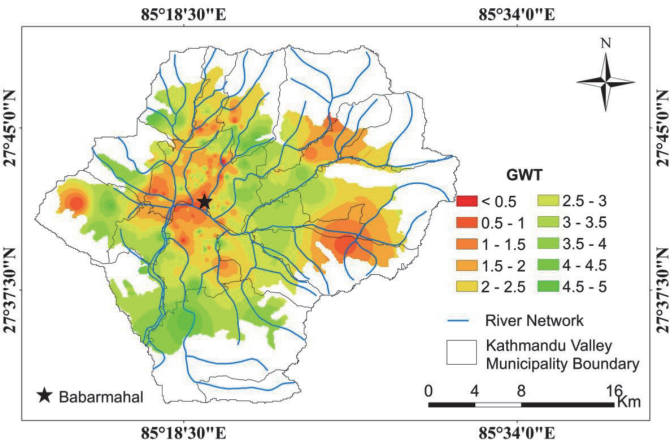


**Fig. 5 GWT contour map of Kathmandu Valley during rainy (monsoon) season**

## 4.2 Predicted Liquefaction Scenario

Previously, attempts were made to map the liquefaction susceptibility of basin deposits of Kathmandu Valley using qualitative and quantitative methods by various authors and institutions in collaboration with the government of Nepal. Widely popular of them are briefly described in the following section.

### 4.2.1 UNDP/UNCHS Liquefaction Susceptibility Map (UNDP/UNCHS 1994)

UNDP/UNCHS map was the first attempt toward liquefaction susceptibility mapping of the Kathmandu basin. It incorpo rated the qualitative method given by Juang and Elton (1991). It is a scoring system based on weightage given to the parameters that influence susceptibility to liquefaction. The project used 6 out of 12 susceptibility factors given by Juang and Elton (1991) for Kathmandu Valley. The factors considered for the study were the depth of water table, capping layer, depth of burial, grain size, age of deposition, and thickness of liquefiable layer. Considering the weightage to each factor and score given to the degree of susceptibility with a very high score of 5 to 1 for low susceptibility, the project categorised four levels of liquefaction susceptibility (*i.e.,* high, medium, low, and very low). The susceptibility map made by UNDP (1994) is given in Fig. 6(b). A high susceptible zone covers about 25% of the study area, 35% by medium, 11% by low, and 29% by low susceptible zone.

### 4.2.2 JICA Liquefaction Potential Map (JICA 2002)

The project carried out as a means of mitigating seismic disasters. They analysed liquefaction using soil physical characteristics, seismic movements, and geological maps of the valley. They made no indication of the number of soil samples analysed. Method adopted a simplified procedure given by Iwasaki *et al.* (1984) with four levels of liquefaction susceptibility (very low, low, moderate, and high). Kathmandu Valley local earthquake scenario was used for the determination of the seismic motion. The susceptibility map by JICA (2002) is presented in Fig. 6(c). It indicates that certain locations near the Bagmati River have a moderate liquefaction risk, while a tiny grid cell to the east has a high liquefaction potential.

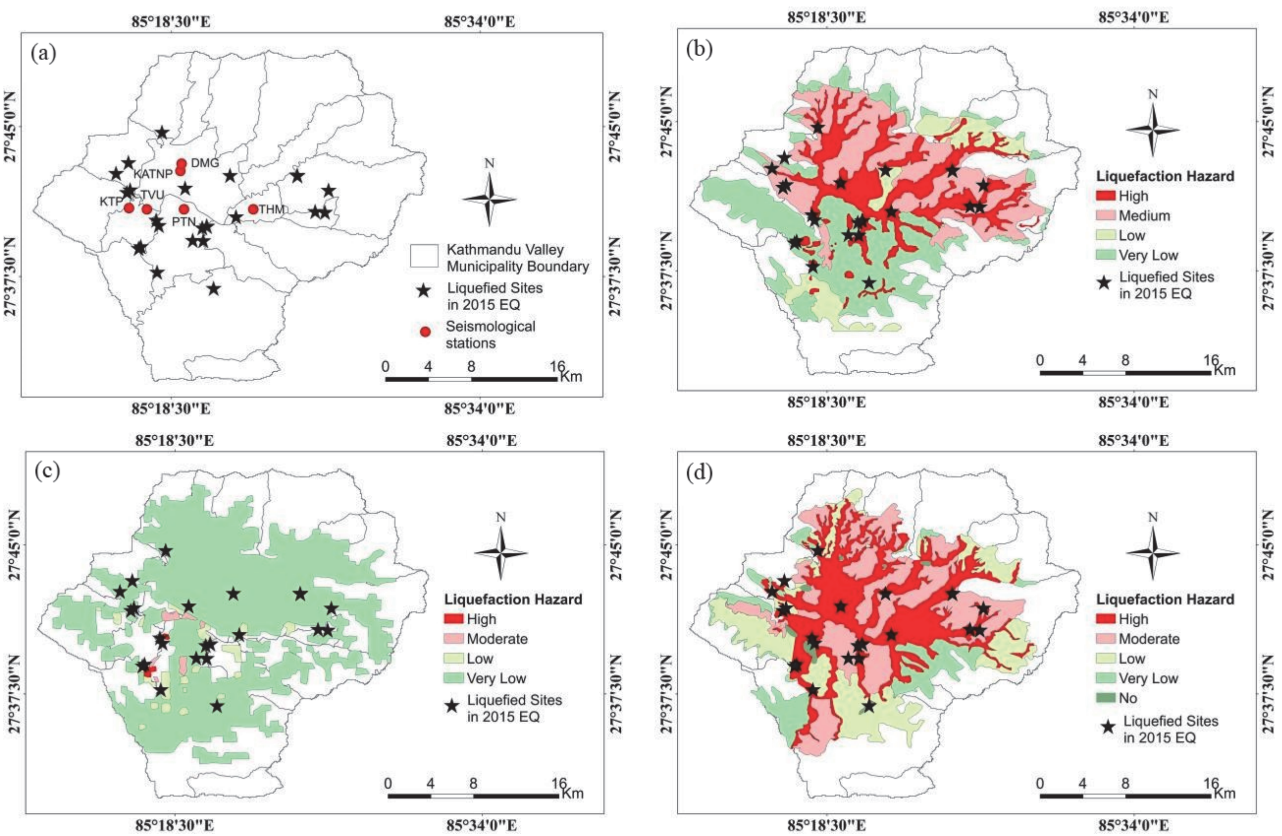


**Fig. 6 (a) Locations of liquefied sites during 2015 Gorkha earthquake, and liquefaction hazard maps prepared by (b) UNDP (1994); (c) JICA (2002); and (d) Piya (2004)**

4.2.3 Liquefaction Susceptibility Map by Piya (Piya 2004)

Liquefaction susceptibility determined based on both quantitative and qualitative analyses. For quantitative analysis, the method given by Seed and Idriss (1971) and Iwasaki *et al.* (1984) were used. Piya (2002) considered topographical and geological data (given by Juang and Elton 1991) for qualitative analysis whereas JICA (2002) neglected topographical and geological parameter (KC *et al.* 2020). This is the reason why Fig. 6(c) is significantly different than Fig. 6(d). A total 328 shallow boreholes were examined for qualitative analysis and 87 boreholes containing geotechnical information were assessed for quantitative study, with all boreholes having a maximum depth of 10 m. The map produced using qualitative analysis validated by quantitatively analysed borehole information. According to the map generated by Piya (2004) (Fig. 6(d)), the region with a high sensitivity to liquefaction accounted for roughly 32% of the total area, primarily along the flood plain and some in the city centre. Roughly 30% of the region has a moderate susceptibility, 25% has a low susceptibility, 12% has a very low susceptibility, and nearly 1% has no liquefaction zone for earthquake scenario of 0.3g PGA.

The comparison of three studies *i.e.,* UNDP (1994), JICA (2002) and Piya (2004) is shown in Table 1.

**Table 1 Comparison of three studies by UNDP (1994), JICA (2002) and Piya (2004)**

| Comparison | UNDP (1994) | JICA (2002) | Piya (2004) |
|---|---|---|---|
| Type of analysis | Qualitative | Quantitative | Qualitative and quantitative |
| Method used | Juang and Elton (1991) | Iwasaki *et al.* (1984) | Seed and Idriss (1971) and Iwasaki *et al.* (1984) |
| Factors/parameter considered | The depth of water table, capping layer, depth of burial, grain size, age of deposition, and thickness of liquefiable layer | Soil physical characteristics, seismic movements, and geological maps of the valley | Seismic, topographical, and geological data |

## 4.3 Observed Liquefaction

4.3.1 1934 Nepal-Bihar Earthquake

The Nepal-Bihar Earthquake (1934, $M_w$8.0) is the largest measured earthquake of Nepalese history with an estimated PGA of 0.3g at Kathmandu, which struck Himalaya on 15 January, 1934. Although the epicentre was about 300 km northeast of the valley, severe building damage with extensive ground fissuring, tilting and sinking was observed in the southeastern part (Chamlagain and Gautam 2015). According to Rana (1935), due to 1934 earthquake, liquefaction was detected in two places inside the Kathmandu Valley, *i.e.,* Tundikhel and Nayabazar (Fig. 7).

4.3.2 2015 Gorkha Earthquake

The ground motion was very much less than the predicted ground motion, and the groundwater table was low. As a result, only six accelerometric stations located within the Kathmandu Valley recorded the 2015 Gorkha earthquake's primary shock (Fig. 6(a)). The EW PGA is maximum (0.192g) at TVU station and minimum (0.150g) at THM and KATNP, whereas NS PGA is maximum (0.246g) at KTP station and minimum (0.124g) at THM station. In UD PGA, the maximum value of 0.206g recorded

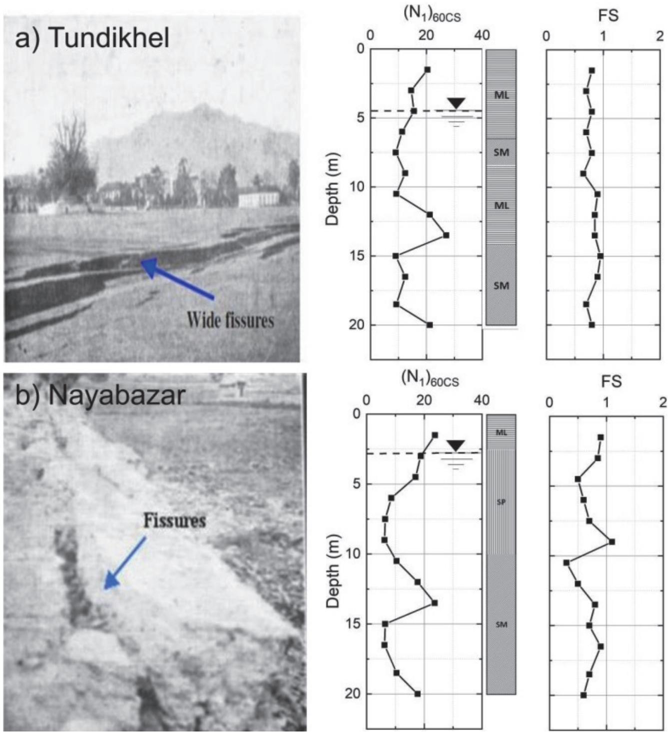


**Fig. 7 Observed liquefaction during 1934 Bihar-Nepal earthquake at (a) Tundikhel and (b) Nayabazar (Rana 1935), with measured SPT, lithology and FS against liquefaction for 0.30g PGA, and $M_w$8.0**

at the DMG station and a minimum of 0.123g at the KTP station. The recorded PGA values in six seismological stations are presented in Table 2.

**Table 2 PGA values recorded for April 25, 2015 Gorkha earthquake (Hough *et al.* 2016)**

| Location | Code | Latitude (N) | Longitude (E) | $PGA_x$ (g) | $PGA_y$ (g) | $PGA_z$ (g) |
|---|---|---|---|---|---|---|
| Bhaktapur | THM | 27.681 | 85.377 | 0.150 | 0.124 | 0.183 |
| Kantipath | KATNP | 27.713 | 85.316 | 0.150 | 0.165 | 0.186 |
| Kirtipur | KTP | 27.682 | 85.273 | 0.153 | 0.246 | 0.123 |
| Lainchaur | DMG | 27.719 | 85.317 | 0.178 | 0.127 | 0.206 |
| Pulchowk | PTN | 27.681 | 85.319 | 0.154 | 0.136 | 0.151 |
| Tribhuvan University | TVU | 27.681 | 85.288 | 0.192 | 0.242 | 0.150 |

The liquefaction occurred at various places in Kathmandu during the 2015 earthquake (Table 3). The total 25 sites, as shown in Fig. 6(a), were liquefied. It was observed that 15 out of 25 liquefied sites were either within or on the Kathmandu Valley edges. Sharma *et al.* (Okamura *et al.* 2015; Gautam *et al.* 2017; Sharma *et al.* 2019). Sharma *et al.* (2019) reported that in communities along the basin's edge, most older structures have been destroyed while modern reinforced concrete structures have been badly damaged. Both geotechnical and structural failures, including liquefaction observed and the high intensity of ground shaking at the basin's border indicates the basin-edge effect's influence. These edge effects generated cyclic stress ratio (CSR) marginally higher than the cyclic resistance ratio of soil (CRR) locally and caused localised liquefaction at the valley edges. The pictures showing liquefaction observations, their borelogs and FS against liquefaction for six selected locations are shown in Figs. 8 and 9.

**Table 3 Details of Liquefied sites caused by 2015 Gorkha earthquake, FS values using Idriss and Boulanger (2008) and LPI values based on Iwasaki *et al.* (1982)**

| Location | Latitude (N) | Longitude (E) | Field observation | FS | LPI |
|---|---|---|---|---|---|
| Bagdol | 27.6676 | 85.2980 | Sand Boils with sand deposits up to few centimetres, pale sand grains | 0.7 ~ 1.7 | 14 |
| Bungamati | 27.6222 | 85.2622 | Sand boiling and fissures with openings 5 to 35 cm wide along the river | 0.6 ~ 2.0 | 25 |
| Changunarayan, NEC | 27.709 | 85.414 | Sand boils, fissures, water well filled up with sand, sand deposits up to few centimetres | 0.5 ~ 2.0 | 13 |
| Duwakot | 27.7094 | 85.4139 | Sand boils and ground fissures | 0.6 ~ 2.0 | 32 |
| Guheshwori | 27.7093 | 85.3576 | Sand boils | < 0.5 | 14 |
| Gwarko | 27.6670 | 85.338 | Sand boils, liquefied and traces of sand | 0.5 ~ 1.0 | 35 |
| Harisiddhi | 27.6549 | 85.3352 | Numerous sand boils | < 0.5 | 15 |
| Hattiban | 27.6668 | 85.3344 | Sand boils and sand deposits up to few centimetres | < 0.5 | 14 |
| Imadol | 27.6668 | 85.3383 | Sand boils and traces of sand | 0.5 ~ 1.5 | 12 |
| Itapakhe | 27.6792 | 85.4289 | Ground fissures and sand boils | 0.8 ~ 1.4 | 35 |
| Jharuwarashi | 27.6151 | 85.3439 | Ground fissures of about 10 cm width and 100 m length | < 0.5 | 36 |
| Kamalvinayak | 27.6785 | 85.4370 | Traces of sand boils | 0.5 ~ 1.0 | 27 |
| Khadka Gaon | 27.6950 | 85.2714 | 500 m long fissures passing through a foundation of residential house | 0.5 ~ 1.3 | 30 |
| Lokanthali | 27.6748 | 85.3626 | Sand boils | < 0.5 | 14 |
| Malpokhari | 27.6720 | 85.2958 | Sand boils with GWT on surface, white and clean sand particles | 0.7 ~ 1.7 | 22 |
| Manamaiju | 27.7453 | 85.3007 | Fissures with the opening of 20 cm width, sand boils and traces | 0.5 ~ 1.8 | 19 |
| Mulpani | 27.7025 | 85.7005 | Ground fissures and sand boils | 0.8 ~ 2.0 | 24 |
| Pakune Pati | 27.6969 | 85.4401 | Sand boils and fissure along the river | < 0.5 | 23 |
| Ramkot | 27.7110 | 85.2622 | Liquefied, a large number of isolated blow sands, clear sand | 0.7 ~ 2.0 | 25 |
| Satdobato | 27.6552 | 85.3264 | Sand boils and ground fissures with up to few cm thickness | < 0.5 | 15 |
| Singhadurbar | 27.6987 | 85.3200 | Sand traces | < 0.5 | 14 |
| Sitapaila | 27.7200 | 85.2726 | Isolated circular sand blows, sands liquefied in three places | 0.5 ~ 0.8 | 13 |
| Syuchatar | 27.6972 | 85.2740 | Traces of sands | 0.5 ~ 1.5 | 23 |
| Taudaha 1 | 27.6499 | 85.2829 | Sand blows in five locations of agricultural field | < 0.5 | 27 |
| Taudaha 2 | 27.6484 | 85.2811 | Sand blows in rice field | 0.5 ~ 1.7 | 21 |

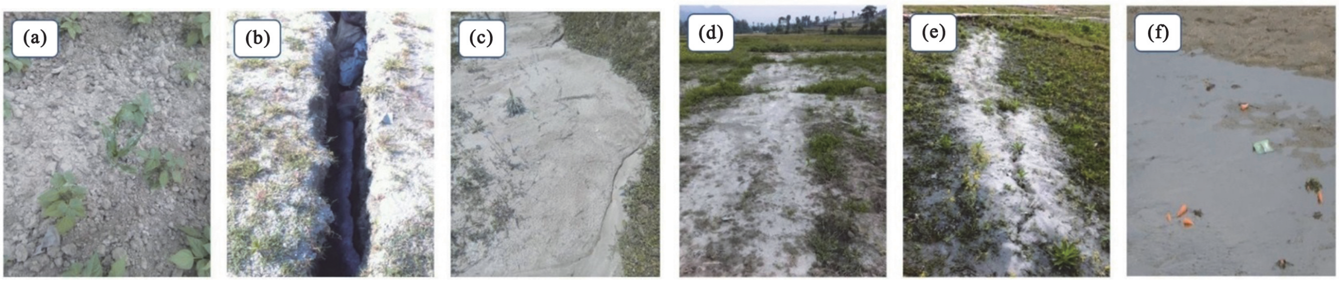


**Fig. 8 Observed liquefaction at (a) Imadol; (b) Manamaiju; (c) Ramkot; (d) Bungmati; (e) Changunarayan NEC, and (f) Mulpani**

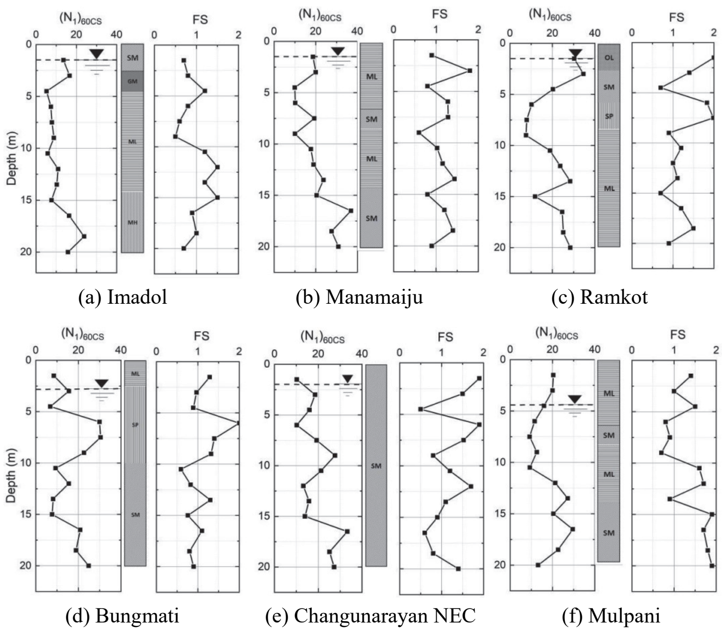


**Fig. 9 Borehole logs calculated $(N_1)_{60CS}$ and FS against liquefaction for 6 liquefied sites during 2015 Gorkha earthquake considering $M_w$7.8 with PGA of 0.18g**

Any serious liquefaction is more likely to occur at locations with an LPI greater than 15 and is improbable at locations with LPI less than 5 (Iwasaki *et al.* 1982; Sonmez 2003). According to Sonmez (2003), liquefaction potential is very high for LPI > 15; high for 5 < LPI ≤ 15; moderate for 2 < LPI ≤ 5; low for 0 < LPI ≤ 2 and non-liquefied for LPI = 0. A typical calculation of LPI is shown in Table 4. Based on LPI calculations for all the boreholes, LPI distribution map is generated for the Kathmandu Valley for two earthquake scenarios of PGA 0.18g ($M_w$7.8) and 0.36g ($M_w$8.4) (Fig. 10). An earthquake scenario of $M_w$7.8 with PGA 0.18g was considered to simulate the 2015 Gorkha earthquake. As the 2015 Gorkha earthquake occurred in April, GWT in dry season was considered. Nepal National Building Code (NBC 2020) has been updated after the 2015 Gorkha earthquake and recommended an earthquake scenario of $M_w$8.4 with PGA 0.36g for Kathmandu Valley. Ground water table in rainy season was considered for the earthquake scenario recommended by NBC (2020). LPI is also assessed for 25 liquefied sites of 2015 Gorkha earthquake and shown in Table 3.

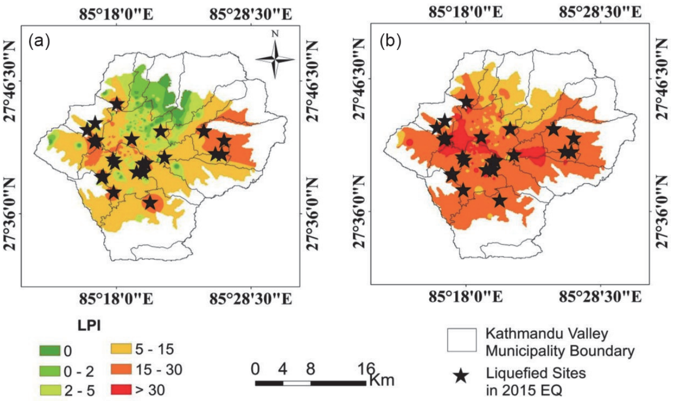


**Fig. 10 LPI map of Kathmandu Valley for earthquake scenarios of (a) $M_w$7.8 with PGA of 0.18g and (b) $M_w$8.4 with PGA of 0.36g**

## 5. DISCUSSIONS

The liquefaction assessment of the Kathmandu Valley with the help of 1510 boreholes data, site reconnaissance and field investigations during 2015 Gorkha earthquake confirms that the valley is highly susceptible to liquefaction. Moreover, the current earthquake scenario and corresponding liquefaction observations indicated that the past studies on liquefaction need revision.

As an example, UNDP (1984) shows that the majority of the Kathmandu Valley has a ‘high’ liquefaction potential, and that susceptibility to liquefaction is classified as very low, low, medium, and high. However, out of 25 liquefied sites in Gorkha earthquake, 8 locations, (*i.e.,* Jharuwarashi, Hattiban, Taudaha, Guheshwori, Sitapaila, Bagdol, Satdobato, and Bungmati) identified as ‘low’ or ‘very low’ susceptible area and 17 locations as ‘medium’ to ‘high’ liquefaction areas (Fig. 6(b)). Liquefaction in Jharuwarashi, Hattiban, Taudaha, Guheshwori, Sitapaila, Bagdol, Satdobato, and Bungmati were observed at lower PGA than designed PGA for Kathmandu valley. This discrepancy may have seen due to three reasons. Firstly, only six factors out of 12 factors as suggested by Juang and Elton (1991) were used during study of liquefaction susceptibility. Moreover, there is no consideration of important geotechnical parameters like SPT-N value, earthquake magnitude, and acceleration in the calculation, which are actually ‘not to miss’ parameters in the assessment of liquefaction. Whereas JICA (2002) shows that most areas of Kathmandu Valley are not susceptible to liquefaction. Over 90% of areas are categorised as ‘very low’ and ‘no’ liquefaction area. Only the flood plain along the rivers is considered a high liquefaction area. As a result, more than 80% of the 2015 Earthquake-caused liquefied sites observed to be in those areas where the JICA study had indicated as ‘no’ liquefaction zone (Fig. 6(c)). The maximum peak ground acceleration of the 2015 Nepal earthquake observed in the valley was approximately 0.18g. Although this acceleration was much smaller than the PGA considered by JICA (2002), extensive soil liquefaction observed at several locations in the valley. It strongly indicates that the liquefaction map prepared by JICA (2002) underestimates the liquefaction susceptibility of the Kathmandu Valley. Likewise, despite having a lesser PGA than that considered by Piya (2004) (*i.e.,* 0.30g), 5 out of 25 locations (*i.e.,* Ramkot, Jharuwarashi, Khadka Gaon, Sitapaila, and Syuchatar) fell under the low liquefaction zone as recommended by Piya (2004) (Fig. 6(d)).

Using simplified procedure proposed by Idriss and Boulanger (2008), the FS against liquefaction of 25 liquefied sites is evaluated and plotted (Table 3). The FS values for different depths observed in between 0.5 to 2, with most of the values being lesser than 1. Moreover, LPI introduced by Iwasaki *et al.* (1982) was calculated for all these sites and tabulated in the same table. It was obtained as high to very high range of susceptibility. Thus, through the study, it is observed that the widely used standard procedure by Idriss and Boulanger (2008) and Iwasaki *et al.* (1982) are effective in liquefaction susceptibility evaluation in Kathmandu Valley for 2015 Gorkha earthquake scenario.

**Table 4 A typical calculation for the estimation of LPI from FS at Babarmahal (as shown in Fig. 5)**

| Depth (m) | SPT-N | $\sigma'_{vc}$ (kPa) | $(N_1)_{60CS}$ | $r_d$ | CSR | MSF | $K_\sigma$ | CRR | FS | $F(z)$ | $W(z)$ | $F(z)\,W(z)$ | LPI |
|---|---|---|---|---|---|---|---|---|---|---|---|---|---|
| 1.5 | 3 | 28.0 | 5.1 | 1.001 | 0.234 | 0.787 | 1.098 | 0.075 | 0.3 | 0.680 | 9.25 | 6.292 | 43 |
| 3.0 | 2 | 42.8 | 3.6 | 0.996 | 0.313 | 0.787 | 1.061 | 0.065 | 0.2 | 0.791 | 8.50 | 6.723 | |
| 4.5 | 1 | 57.6 | 1.7 | 0.990 | 0.350 | 0.787 | 1.036 | 0.056 | 0.2 | 0.840 | 7.75 | 6.507 | |
| 6.0 | 10 | 72.4 | 14.0 | 0.983 | 0.370 | 0.787 | 1.036 | 0.121 | 0.3 | 0.674 | 7.00 | 4.719 | |
| 7.5 | 2 | 87.2 | 2.6 | 0.975 | 0.382 | 0.787 | 1.010 | 0.058 | 0.2 | 0.848 | 6.25 | 5.299 | |
| 9.0 | 15 | 102.0 | 18.7 | 0.966 | 0.389 | 0.787 | 0.999 | 0.150 | 0.4 | 0.615 | 5.50 | 3.382 | |
| 10.5 | 5 | 116.9 | 5.7 | 0.957 | 0.393 | 0.787 | 0.989 | 0.070 | 0.2 | 0.821 | 4.75 | 3.900 | |
| 12.0 | 16 | 131.7 | 17.7 | 0.946 | 0.395 | 0.787 | 0.968 | 0.138 | 0.3 | 0.651 | 4.00 | 2.605 | |
| 13.5 | 19 | 146.5 | 20.2 | 0.935 | 0.395 | 0.787 | 0.950 | 0.156 | 0.4 | 0.606 | 3.25 | 1.969 | |
| 15.0 | 18 | 161.3 | 18.2 | 0.923 | 0.393 | 0.787 | 0.942 | 0.137 | 0.3 | 0.651 | 2.50 | 1.627 | |

## 6. CONCLUSIONS

The authors reached to following conclusions from this study:

- At the majority of locations, non-plastic silts or fine sand ejected onto the agricultural fields, producing deposits as thin as a few millimetres. There was little evidence of liquefaction caused damage to building infrastructures next to liquefied regions.
- Liquefaction manifested by the Gorkha Earthquake (2015, $M_w$7.8) was limited and localized. It might be ascribed to existing lacustrine soils, low amplitude motions, and deep groundwater table during the earthquake.
- Although PGA observed during the earthquake in the valley was much smaller than expected and groundwater level was deep due to dry season, in many localised places, significant soil liquefaction was reported in Kathmandu Valley. It highlights that the valley is highly prone to liquefaction and liquefaction assessment is essential for seismic hazard mitigation.
- The existing hazard maps by UNDP (1994), JICA (2002) and Piya (2004) found unrepresentative and underestimated the liquefaction susceptibility of Kathmandu Valley. Out of three, the liquefaction map prepared by Piya (2004) was found most reliable, whereas JICA (2002) was the least.
- The standard simplified procedure propounded by Idriss and Boulanger (2008) to assess liquefaction potential of the area found valid in Nepal scenario.
- Comprehensive geotechnical investigations using shear wave velocity test should be carried out to investigate the soil's seismic reaction and to consider reconstruction works, urban planning, and development plan in the valley.
- It is recommended that hazard maps should be revised recognizing local site effects, ground amplification, and the current groundwater level. More studies on soil conditions and response to the strong motion records at several sites are necessary. Hospitals, schools, fire and police stations, lifeline services, and public buildings, particularly those built over unstable soils which might liquefy even with mild shaking, ought to be moved or renovated to ensure that they continue to function during an earthquake.

## ACKNOWLEDGEMENTS

The first author sincere acknowledges the support received from Nepal Academy of Science and Technology (NAST) for the PhD Fellowship and the research guidance obtained through the Geo-Engineering and Geoscience Research Accelerator (GeoRA) program from BGC Engineering Inc. (Vancouver, Canada). The secondary borehole data and related information used in this work were obtained from various local organizations including Soil Test Pvt. Ltd., Pashupati Drillers, Multi Lab Pvt. Ltd., Clay Engineering, Archiplan Pvt. Ltd., Adarsha Design and Solutions Pvt. Ltd. We appreciate the help of Mr. Rajan K.C. (Post-Graduate Student, Institute of Engineering, Pulchowk Campus, Tribhuvan University, Nepal) in preparing some of the maps used in this paper.

## FUNDING

The authors did not receive any funding for this research.

## DATA AVAILABILITY

The datasets used and/or analysed during this work are accessible upon reasonable request from the corresponding author.

## DECLARATION OF INTEREST STATEMENT

No possible conflicts of interest were disclosed by the authors.

## REFERENCES

Bray, J.D. and Sancio, R.B. (2006). "Assessment of the liquefaction susceptibility of fine-grained soils." *Journal of Geotechnical and Geoenvironmental Engineering*, **132**(9), 1165-1177. https://doi.org/10.1061/(ASCE)1090-0241(2006)132:9(1165)

Casagrande, A. (1947). "Classification and identification of soils." *Proc., American Society of Civil Engineers*, **73**(6), 783-810. https://doi.org/10.1061/TACEAT.0006109

Chamlagain, D. and Gautam, D. (2015). "Seismic hazard in the himalayan intermontane basins: An example from Kathmandu Valley, Nepal." *Springer Japan 2015*, Issue October. https://doi.org/10.1007/978-4-431-55242-0_5

Copeland, P. (1997). "The when and where of the growth of the Himalaya and the Tibetan Plateau." *Tectonic Uplift and Climate Change*, 19-40, Springer. https://doi.org/10.1007/978-1-4615-5935-1_2

Gautam, D., de Magistris, F.S., and Fabbrocino, G. (2017). "Soil liquefaction in Kathmandu Valley due to 25 April 2015 Gorkha, Nepal earthquake." *Soil Dynamics and Earthquake Engineering*, **97**, 37-47. https://doi.org/10.1016/j.soildyn.2017.03.001

Hough, S.E., Martin, S.S., Gahalaut, V., Joshi, A., Landes, M., and Bossu, R. (2016). "A comparison of observed and predicted ground motions from the 2015 $M_w$ 7.8 Gorkha, Nepal, earthquake." *Natural Hazards*, **84**(3), 1661-1684. https://doi.org/10.1007/s11069-016-2505-8

Idriss, I.M. and Boulanger, R.W. (2008). *Soil Liquefaction During Earthquakes*. Earthquake Engineering Research Institute.

Iwasaki, T., Arakawa, T., and Tokida, K.-I. (1984). "Simplified procedures for assessing soil liquefaction during earthquakes." *International Journal of Soil Dynamics and Earthquake Engineering*, **3**(1), 49-58. https://doi.org/10.1016/0261-7277(84)90027-5

Iwasaki, T., Tokida, K. I., Tatsuoka, F., Watanabe, S., Yasuda, S., and Sato, H. (1982). "Microzonation for soil liquefaction potential using simplified methods." *Proc., 3rd International Conference on Microzonation*, Seattle, **3**(2), 1310-1330.

Jha, S.K., Karki, B., and Bhattarai, A. (2020). "Deterministic and probabilistic evaluation of liquefaction potential: A case study from 2015 Gorkha (Nepal) Earthquake." *Geotechnical and Geological Engineering*, **38**(4), 4369-4384. https://doi.org/10.1007/s10706-020-01277-7

JICA (2002). *The Study on Earthquake Disaster Mitigation in the Kathmandu Valley, Kingdom of Nepal*, Japan International

Cooperation Agency (JICA) and Ministry of Home Affairs (MOHA), Tokyo.

Juang, C.H. and Elton, D.J. (1991). "Use of fuzzy sets for liquefaction susceptibility zonation." *Proc., Fourth International Conference on Seismic Zonation*, **2**, 629-636.

KC, A., Sharma, K., and Pokharel, B. (2019). "Performance of heritage structure in Kathmandu Valley during 2015 Gorkha Nepal earthquake." *Journal of Earthquake Engineering*, **23**(8), 1346-1384. https://doi.org/10.1080/13632469.2017.1360225

KC, S., Bhochhibhoya, S., Adhikari, P., Adhikari, P., and Gautam, D. (2020). "Probabilistic seismic liquefaction hazard assessment of Kathmandu valley, Nepal." *Geomatics, Natural Hazards Risk*, **11**(1), 259-271. https://doi.org/10.1080/19475705.2020.1718220

Koseki, J., Wakamatsu, K., Sawada, S., and Matsushita, K. (2015). "Liquefaction-induced damage to houses and its countermeasures at Minami-Kurihashi in Kuki City during the 2011 Tohoku Earthquake, Japan." *Soil Dynamics and Earthquake Engineering*, **79**, 391-400. https://doi.org/10.1016/j.soildyn.2015.07.014

Moribayashi, S. and Maruo, Y. (1980). "Basement topography of the Kathmandu Valley, Nepal." *Journal of The Japan Society of Engineering Geologist*, **21**(2), 30-37. https://doi.org/10.5110/jjseg.21.80

Okamura, M., Bhandary, N.P., Mori, S., Marasini, N., and Hazarika, H. (2015). "Report on a reconnaissance survey of damage in Kathmandu caused by the 2015 Gorkha Nepal earthquake." *Soils Found*, **55**(5), 1015-1029. https://doi.org/10.1016/j.sandf.2015.09.005

Pathak, D.R., Hiratsuka, A., Awata, I., and Chen, L. (2009). "Groundwater vulnerability assessment in shallow aquifer of Kathmandu Valley using GIS-based DRASTIC model." *Environmental Geology*, **57**(7), 1569-1578. https://doi.org/10.1007/s00254-008-1432-8

Piya, B.K. (2004). "Generation of a geological database for the liquefaction hazard assessment in Kathmandu Valley." *Geo-Information Science*, March, 141.

Rana, B. S. (1935). *Nepal ko Maha Bhukampa (The Great Earthquake of Nepal)*. Jorganesh Press, Kathmandu, **1**, 250 (in Nepali).

Sakai, H. (2001). "Stratigraphic division and sedimentary facies of the Kathmandu Basin Group, central Nepal." *Journal of Nepal Geological Society*, **25**(Sp. Issue), 19-32. https://doi.org/10.3126/jngs.v25i0.32043

Sakai, H, Fujii, R., and Kuwahara, Y. (2002). "Changes in the depositional system of the Paleo-Kathmandu Lake caused by uplift of the Nepal Lesser Himalayas." *Journal of Asian Earth Sciences*, **20**(3), 267-276. https://doi.org/10.1016/S1367-9120(01)00046-3

Seed, H.B. and Idriss, I.M. (1971). "Simplified procedure for evaluating soil liquefaction potential." *Journal of Soil Mechanics & Foundations Div.*, **97**(9), 1249-1273. https://doi.org/10.1061/JSFEAQ.0001662

Sharma, K., Deng, L., and Khadka, D. (2019). "Reconnaissance of liquefaction case studies in 2015 Gorkha (Nepal) earthquake and assessment of liquefaction susceptibility." *International Journal of Geotechnical Engineering*, **13**(4), 326-338. https://doi.org/10.1080/19386362.2017.1350338

Sharma, K., Deng, L., and Noguez, C.C. (2016). "Field investigation on the performance of building structures during the April 25, 2015, Gorkha earthquake in Nepal." *Engineering Structures*, **121**, 61-74. https://doi.org/10.1016/j.engstruct.2016.04.043

Sharma, K., KC, A., and Pokharel, B. (2018). "Challenges for reconstruction after $M_w$ 7.8 Gorkha earthquake: A study on devastated area of Nepal." *Geomatics, Natural Hazards and Risk*, **9**(1), 760-790. https://doi.org/10.1080/19475705.2018.1480535

Sharma, K., KC, A., Subedi, M., and Pokharel, B. (2018). "Post disaster reconstruction after 2015 Gorkha earthquake: Challenges and influencing factors." *Journal of the Institute of Engineering*, **14**(1), 52-63. https://doi.org/10.3126/jie.v14i1.20068

Sharma, K., Subedi, M., Acharya, I., and Pokharel, B. (2017). "Geotechnical and Structural Aspect of 2015 Gorkha Nepal Earthquake and Lesson Learnt." *Journal of the Institute of Engineering*, **13**(1), 20-36. https://doi.org/10.3126/jie.v13i1.20345

Sharma, K., Subedi, M., Parajuli, R.R., and Pokharel, B. (2017). "Effects of surface geology and topography on the damage severity during the 2015 Nepal Gorkha earthquake." *Lowland Technology International*, **18**(4), 269-282.

Shrestha, S., Semkuyu, D.J., and Pandey, V.P. (2016). "Assessment of groundwater vulnerability and risk to pollution in Kathmandu Valley, Nepal." *Science of the Total Environment*, **556**, 23-35. https://doi.org/10.1016/j.scitotenv.2016.03.021

Sonmez, H. (2003). "Modification of the liquefaction potential index and liquefaction susceptibility mapping for a liquefaction-prone area (Inegol, Turkey)." *Environmental Geology*, **44**(7), 862-871. https://doi.org/10.1007/s00254-003-0831-0

Subedi, M., K.C., Rajan, and Acharya, I.P. (2021). "SPT-based seismic soil liquefaction potential evaluation of Kathmandu Valley using first-order second-moment method." *GeoNiagara 2021*, Canada.

Subedi, M., Sharma, K., Acharya, I.P., and Adhikari, K. (2016). "Liquefaction of soil in Kathmandu Valley from the 2015 Gorkha, Nepal, Earthquake." *Technical Journal Special Issue on Gorkha Earthquake 2015*, **1**, 108-116.

Subedi, M., Sharma, K., Acharya, I.P., and Adhikari, K. (2018). "Soil liquefaction in Kathmandu Valley due to 2015 Gorkha, Nepal Earthquake and assessment of liquefaction susceptibility." *Proc., 11th National Conference on Earthquake Engineering*, Los Angeles, USA.

Thapa, D.R., Tao, X., Wang, G., and Fan, F. (2017). "Deterministic seismic hazard assessment for Nepal." *Proc., 16th World Conference on Earthquake Engineering (16WCEE-2017)*, Santiago, Chile, Paper No. 730.

Tsuchida, H. and Hayashi, S. (1972). *Estimation of Liquefaction Potential of Sandy Soils*, Publication of McGraw Hill Book Company, **14**.

UNDP/HMG/UNCHS (1994). *Seismic Hazard Mapping and Risk Assessment for Nepal*.

Yoshida, M. (1984). "Neogene to Quaternary lacustrine sediments in the Kathmandu Valley, Nepal." *Journal of Nepal Geological Society*, **4**, 73-100.